



Solvability of chaotic fractional systems with 3D four-scroll attractors



Emile Franc Doungmo Goufo

Department of Mathematical Sciences, University of South Africa, Florida, 0003, South Africa

ARTICLE INFO

Article history:

Received 2 July 2017

Revised 31 August 2017

Accepted 31 August 2017

MSC:

26A33

65C20

65L20

26A36

33F05

Keywords:

Fractional system

Haar wavelet numerical

Strange attractors

Chaotic multi-wing attractor

Convergence

ABSTRACT

One of the questions that has recently predominated the literature is the generation and modulation of strange chaotic attractors, namely the ones with multi scrolls. The fractional theory might be useful in addressing the questions. We use the Caputo fractional derivative together with Haar wavelet numerical scheme to investigate a three-dimensional system that generates chaotic four-wing attractors. Some conditions of stability at the origin (the trivial equilibrium point) are provided for the model. The error analysis shows that the method converges and is concluded thanks to Fubini–Tonelli theorem for non-negative functions and the Mean value theorem for definite integrals. Graphical simulations, performed for some different value of the derivative order α show existence, as expected, of chaotic dynamics characterized by orbits with four scrolls, typical to strange attractors. Hence, fractional calculus appears to be useful in generating and modulating chaotic multi-wing attractors.

© 2017 Elsevier Ltd. All rights reserved.

1. Introduction to the model

Even though a huge interest for fractional differentiations and their properties has only resurfaced during the last two decades, fractional calculus remains a scientific domain as old integer order calculus is. Many authors have applied it in various processes related to real life phenomena, such as acoustic dissipation, viscoelastic systems, mathematical epidemiology, continuous time random walk, biomedical engineering, porous media, control theory, Levy statistics, fractional Brownian, dielectric polarization, fractional signal and image processing, electrolyte/electrolyte polarization, fractional filters motion and nonlocal phenomena [1–9]. Most of the models used in those analysis are non linear and require sophisticated techniques to solve them. Hence, number of numerical methods for the solution of fractional differential equations have been developed and proposed in numerous works, in order to provide an improved description of the phenomenon under investigation. Common numerical methods include finite difference method, variational iteration method, Crank–Nicholson method, adomian or homotopy analysis and lastly the one of our interest in this paper: wavelet method [10–18]. Wavelet analysis appears to be relatively new in mathematical analysis theory but is catching interest among scientist, especially those specialized in

fluid flow, applied in signal and image manipulation and numerical analysis, etc.

On the other side, the scientific academy has seen, during the years, the development and simulation of the so called strange attractors whose unique particularity is to exhibit attractor with a fractal structure [19–21]. Edward Lorenz [22] is one of the first to propose strange attractor, Lorenz attractor. However, there are number of other systems of equations that generate strange attractors leading to chaotic dynamics. Few examples include the Rössler attractor [23] and Hénon attractor [24], Arneodo Attractor [25], Lu-chen attractor [26], etc, and lastly the one of our interest in this paper: Four-wing attractor. This paper aims to assess the effect resulted from a combination of fractional derivative and those strange systems of equations. Whence, the whole analysis conducted here consists of exploring the existence of four-wing attractor and stability results for the model (1.3) here below, that belongs to the same family as the chaotic Rössler system [23,27,28] given as

$$\begin{cases} \frac{d}{dt}x(t) = -y - z, \\ \frac{d}{dt}y(t) = x + ay, \\ \frac{d}{dt}z(t) = bx + z(x - c), \end{cases} \quad (1.1)$$

E-mail addresses: dgoufef@unisa.ac.za, franckemile2006@yahoo.ca

or the Lorenz system [22,27,28]

$$\begin{cases} \frac{d}{dt}x(t) = \sigma(y - x), \\ \frac{d}{dt}y(t) = x(\rho - z) - y, \\ \frac{d}{dt}z(t) = xy - \delta z, \end{cases} \quad (1.2)$$

with $\alpha \in [0; 1]$, $\beta \in (0, +\infty)$, $t > 0$ where $x = x(t)$, $y = y(t)$, $z = z(t)$ represent the system state and σ, ρ, δ are real constants parameterizing the system.

The model of our interest reads as

$$\begin{cases} D_t^\alpha x(t) = ax + cyz, \\ D_t^\alpha y(t) = bx + dy - xz, \\ D_t^\alpha z(t) = ez + fxy, \end{cases} \quad (1.3)$$

where $a, b, d, e \in \mathbb{R}$, $c > 0$ and $f < 0$ with $cf \neq 0$. $x = x(t)$, $y = y(t)$, $z = z(t)$ represent the system state and a_1, a_2, b_1, c_1 are real constants parameterizing the system. The term D_t^α represents a fractional derivative. In the next section, a comprehensive definition of the fractional derivative we employ, namely the Caputo derivative and more other details with properties are provided. Our approach is to fully analyze the model (1.3) for any order $\alpha \in [0; 1]$. More precisely, we solve the model using the numerical method of Haar wavelets that is described in Section 3 below. The goal is to refute or not the (non)existence of a chaotic four-wing attractor for (1.3). Before that, let us recall the following

Theorem 1.1. *It is impossible for the system (1.3) to generate a chaotic four-wing attractor when $\alpha = 1$ and $b = 0$.*

Proof. The proof follows from [28, Theorem 1] and the fact that

$$D_t^1 u(t) \sim \frac{du(t)}{dt}. \quad (1.4)$$

□

Hence for $\alpha = 1$, the model (1.3) reduces to the system

$$\begin{cases} x'(t) = ax + cyz, \\ y'(t) = bx + dy - xz, \\ z'(t) = ez + fxy \end{cases} \quad (1.5)$$

System (4.2) was introduced in [28,29] proved to be chaotic in the same level as Lorenz or Rössler equations are. Moreover, it generates a four-wing chaotic attractor with less terms in the system equations compared to other models. Then, let us analyze the extended model (1.3) and exhibit the shape of the solutions in order to compare with those of (4.2).

2. A note on derivative with non-integer order [11,27,30–33]

In this particular domain of calculus, the most popular definitions of derivatives with non-integer order remain the Riemann–Liouville derivative (RLFD) and Caputo derivative. The first was named after the work of Bernhard Riemann and Joseph Liouville more than a century and a half ago. Their main idea started with the following integral of order α

$$I^\alpha f(t) = \frac{1}{\Gamma(\alpha)} \int_a^t \frac{f(\tau)}{(t - \tau)^{1-\alpha}} d\tau \quad (2.1)$$

based on Euler transform when applied to analytic function and Cauchy’s formula for calculating iterated integrals. Hence, the RLFD of order α was defined for any $t > 0$ as

$$D_t^\alpha f(t) = \frac{d^n}{dt^n} I^{n-\alpha} f(t), \quad n - 1 < \alpha \leq n \quad (2.2)$$

where $n \in \mathbb{N}$, $-\infty \leq a < t$, $b > a$ and $f : (a, b) \rightarrow \mathbb{R}$ an arbitrary real and locally integrable function. After that, in 1967, Michele Caputo proposed another definition closely related to the previous one and given (for $n = 1$) as

$$D_t^\alpha f(t) = I^{1-\alpha} \frac{d}{dt} f(t), \quad 0 < \alpha \leq 1 \quad (2.3)$$

where the unknowns are the same as in (2.2), except the function f that is from the first order Sobolev space

$$H^1(a, b) = \left\{ f : f, \frac{d}{dt} f \in L^2(a, b) \right\}. \quad (2.4)$$

Recently, more investigations conducted by Caputo and Fabrizio [31] pointed out another definition, the Caputo–Fabrizio fractional derivative given by

$${}^{cf}D_t^\alpha f(t) = \frac{M(\alpha)}{(1-\alpha)} \int_0^t \dot{f}(\tau) \exp\left(-\frac{\alpha(t-\tau)}{1-\alpha}\right) d\tau, \quad (2.5)$$

where $M(\alpha)$ is a normalization function such that $M(0) = M(1) = 1$. Soon after that Losada and Nieto [32] improved this definition as

$${}^{cf}D_t^\alpha f(t) = \frac{(2-\alpha)M(\alpha)}{2(1-\alpha)} \int_0^t \dot{f}(\tau) \exp\left(-\frac{\alpha(t-\tau)}{1-\alpha}\right) d\tau. \quad (2.6)$$

and defined a more suitable fractional integral that reads as:

$${}^{cf}I_t^\alpha f(t) = \frac{2(1-\alpha)}{(2-\alpha)M(\alpha)} f(t) + \frac{2\alpha}{(2-\alpha)M(\alpha)} \int_0^t f(\tau) d\tau, \quad (2.7)$$

$\alpha \in [0, 1]$ $t \geq 0$. This anti-derivative represents sort of average between the function f and its integral of order one. In the same momentum, Goufo and Atangana [4,11] propose the New Riemann–Liouville fractional order derivative given for $\alpha \in [0, 1]$ by

$${}_a\mathcal{D}_t^\alpha f(t) = \frac{M(\alpha)}{1-\alpha} \frac{d}{dt} \int_a^t f(\tau) \exp\left(-\frac{\alpha}{1-\alpha}(t-\tau)\right) d\tau \quad (2.8)$$

Again, the NRLFD is without any singularity at $t = \tau$ in comparison to the classical Riemann–Liouville fractional order derivative (2.2) and also it verifies

$$\lim_{\alpha \rightarrow 1} {}_a\mathcal{D}_t^\alpha f(t) = \dot{f}(t) \quad (2.9)$$

and

$$\lim_{\alpha \rightarrow 0} {}_a\mathcal{D}_t^\alpha f(t) = f(t). \quad (2.10)$$

In order to address the issue of locality that exists in the above definitions of fractional derivatives, nonlocal definitions were proposed and generalized [27,33] as follows: Let f be a function in $H^1(a, b)$; $b > a$; $\alpha \in [0; 1]$, $\beta \in (0, +\infty)$ then, the Caputo-sense one-parameter and nonlocal fractional derivative of order α is given by:

$${}^{ab}D_t^\alpha f(t) = \frac{M(\alpha)}{(1-\alpha)} \int_a^t \dot{f}(\tau) E_\alpha \left[-\frac{\alpha(t-\tau)^\alpha}{1-\alpha} \right] d\tau = {}^{abc}D_t^\alpha f(t). \quad (2.11)$$

where $M(\alpha)$ is the same normalization function defined in (2.5) and E_α the one-parameter Mittag–Leffler function.

The Caputo-sense two-parameter and nonlocal fractional derivative of order α knowing β as a parameter is given by:

$${}^{gc}D_t^{\alpha,\beta} f(t) = \frac{\beta W(\alpha, \beta)}{(\beta-\alpha)} \int_a^t \dot{f}(\tau) (t-\tau)^{\beta-1} E_{\alpha,\beta} \left[-\frac{\alpha\beta(t-\tau)^\alpha}{\beta-\alpha} \right] d\tau, \quad (2.12)$$

where $W(\alpha, \beta)$ is a two-variable normalization function such that $W(0, 1) = W(1, 1) = 1$, and $E_{\alpha, \beta}$ the two-parameter Mittag–Leffler function.

The Laplace transform of the later definition is given by

$$\mathcal{L}({}^c D_t^\alpha f(t), s) = \frac{M(\alpha) s^\alpha \tilde{f}(x, s) - s^{\alpha-1} f(0)}{(1-\alpha) s^\alpha + \frac{\alpha}{1-\alpha}} \tag{2.13}$$

where $\tilde{f} = \mathcal{L}(f(t), s)$.

3. A note on Haar wavelets

The function

$$H(t) = \begin{cases} 1, & \text{for } t \in [0, 1/2); \\ -1, & \text{for } t \in [1/2, 1); \\ 0, & \text{elsewhere.} \end{cases} \tag{3.1}$$

that is defined on the real line \mathbb{R} is called the Haar wavelet [16–18]. Let $t \in [0, 1)$, define for each $i = 0, 1, 2, 3, \dots$ the family

$$h_i(t) = \begin{cases} 2^{\frac{j}{2}} H(2^j t - k), & \text{for } i = 1, 2, \dots; \\ 1, & \text{for } i = 0, \end{cases} \tag{3.2}$$

where we keep in mind the remark that each $i = 0, 1, 2, \dots$ can be written into the form $i = 2^j + k$ with $j = 0, 1, 2, \dots$ and $k = 0, 1, 2, \dots, 2^j - 1$. Hence, it can be proved that resulting family $\{h_i(t)\}_{i=0}^\infty$ forms a complete orthonormal system in the Banach space of square-integrable function $L^2[0, 1)$. Moreover, if we consider the function r taking in the Banach space of continuous functions $C[0, 1)$ then, the series $\sum_{i=0}^\infty \langle r, h_i \rangle h_i$ converges uniformly to r with $\langle r, h_i \rangle = \int_0^1 r(t) h_i(t) dt$. We can then decompose the same function r to have

$$r(t) = \sum_{i=0}^\infty c_i h_i(t)$$

where $c_i = \langle r, h_i \rangle$. For reasons of practicability, the approximated solution reads as

$$r(t) \approx r_k(t) = \sum_{i=0}^{k-1} c_i h_i(t)$$

where $k \in \{2^j : j = 0, 1, 2, \dots\}$.

Let $b \in \mathbb{N}$, we are now making use of the translation of the haar function on $[0, b)$ to define the function

$$h_{s,i}(t) = h_i(t - s + 1) \quad s = 1, 2, \dots, b \quad \text{and} \quad i = 0, 1, 2, \dots \tag{3.3}$$

where h_i is given by (3.2). Obviously the same properties that hold for h_i also hold for $h_{s,i}$. Namely, the family $\{h_{s,i}(t)\}_{i=0}^\infty$, ($s = 1, 2, \dots, b$) forms a complete orthonormal system in the Banach space of square-integrable function $L^2[0, b)$. Hence it is also possible to exploit the following haar orthonormal basis functions

$$c_{s,i} = \langle r, h_{s,i} \rangle = \int_0^b r(t) h_{s,i}(t) dt$$

to expand the solution $r \in L^2[0, b)$ as the series

$$r(t) = \sum_{s=1}^b \sum_{i=0}^\infty c_{s,i} h_{s,i}(t). \tag{3.4}$$

Similarly for reasons of practicability, the approximated solution reads as

$$r(t) \approx r_k(t) = \sum_{s=1}^b \sum_{i=0}^{k-1} c_{s,i} h_{s,i}(t) \tag{3.5}$$

where $k \in \{2^j : j = 0, 1, 2, \dots\}$. Note that (3.5) can be expressed into the compact form

$$r(t) \approx r_k(t) = {}^T \mathbf{C}_{bk \times 1} \mathbf{H}_{bk \times 1} \tag{3.6}$$

where ${}^T \mathbf{C}_{bk \times 1}$ is the transpose vector of

$$\mathbf{C}_{bk \times 1} = \begin{pmatrix} c_{1,0} \\ \vdots \\ c_{1,k-1} \\ c_{2,0} \\ \vdots \\ c_{2,k-1} \\ \vdots \\ c_{b,0} \\ \vdots \\ c_{b,k-1} \end{pmatrix} \quad \text{and} \quad \mathbf{H}_{bk \times 1} = \begin{pmatrix} h_{1,0} \\ \vdots \\ h_{1,k-1} \\ h_{2,0} \\ \vdots \\ h_{2,k-1} \\ \vdots \\ h_{b,0} \\ \vdots \\ h_{b,k-1} \end{pmatrix}.$$

4. Model analysis

The equilibrium points of model of system (1.3) are obtained via the system

$$\begin{cases} 0 = D_t^\alpha x(t) = ax + cyz, \\ 0 = D_t^\alpha y(t) = bx + dy - xz, \\ 0 = D_t^\alpha z(t) = ez + fxy, \end{cases} \tag{4.1}$$

For $e > 0$, $\frac{ea}{cf} > 0$, $b^2c - 4ad > 0$, obviously $E_0 = (0, 0, 0)$ is the trivial equilibrium point and we have four non-trivial other equilibrium points given by

$$\begin{aligned} E_{1,2} &= \left(\frac{1}{a} ce^{\frac{1}{2}} \left(\mp b + \sqrt{\frac{1}{c}(b^2c - 4ad)} \right) \sqrt{\frac{a}{cf}}, \pm \sqrt{\frac{ea}{cf}}, \right. \\ &\quad \left. \frac{1}{2} \left(b \mp \sqrt{\frac{1}{c}(b^2c - 4ad)} \right) \right), \\ E_{3,4} &= \left(-\frac{1}{2a} ce^{\frac{1}{2}} \left(\pm b + \sqrt{\frac{1}{c}(b^2c - 4ad)} \right) \sqrt{\frac{a}{cf}}, \pm \sqrt{\frac{ea}{cf}}, \right. \\ &\quad \left. \frac{1}{2} \left(b \pm \sqrt{\frac{1}{c}(b^2c - 4ad)} \right) \right). \end{aligned} \tag{4.2}$$

Remark 4.1.

1. This clearly insinuates that model (1.3) with the five equilibrium points $E_{0,1,2,3,4}$ cannot be topologically equivalent to the Lorenz model with its three maximum equilibrium points [27,28,34].
2. The model (1.3) has no non-trivial other equilibrium points if $\frac{ea}{cf} > 0$, or $b^2c - 4ad > 0$.

4.1. Conditions around the stability of the origin $E_0 = (0, 0, 0)$ when $0 \leq \alpha < 1$

To have a look at the stability of the trivial equilibrium point $E_0 = (0, 0, 0)$ of the model (1.3), we evaluated at E_0 , the Jacobian matrix $J(E_0)$ for the system given that reads as follows:

$$J(E_0) = Df(E_0) = \begin{pmatrix} a & 0 & 0 \\ b & d & 0 \\ 0 & 0 & e \end{pmatrix} \tag{4.3}$$

We know, see [35], that the trivial equilibrium point $E_0 = (0, 0, 0)$ for a fractional model of type (1.3) is asymptotically stable if all of the eigenvalues, $\lambda_{1,2,3}$ of $J(E_0)$ satisfy the following constraint:

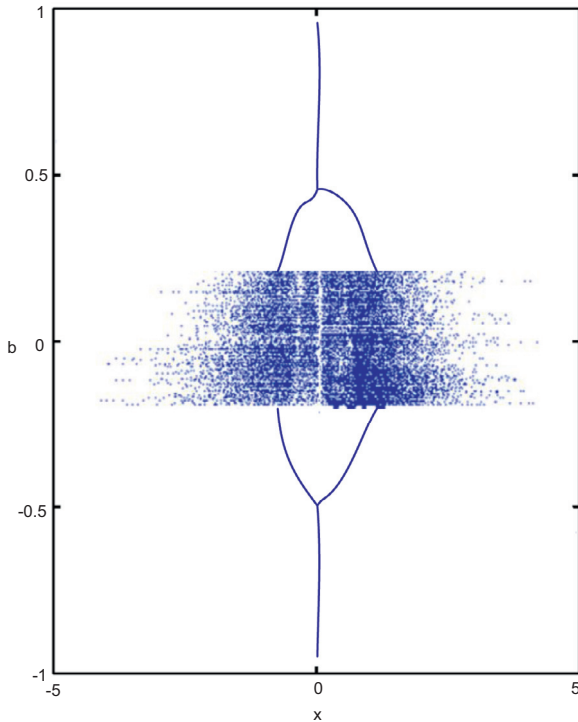


Fig. 1. Bifurcation diagram of system state x versus the parameter b , for the control parameters $a = 0.25$, $c = 1$, $d = -0.45$, $e = -1$, $f = -1$ and $\alpha = 1.0$. It shows the huge importance of parameter b in creating a multi-wing attractor.

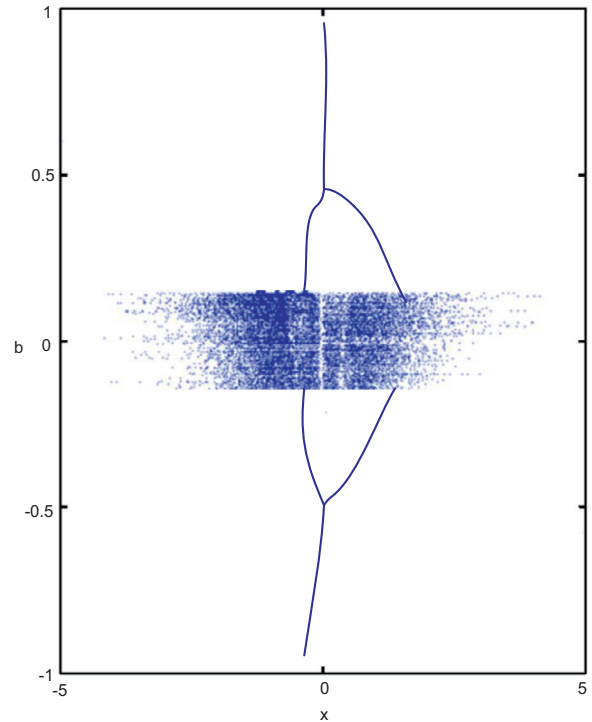


Fig. 2. Bifurcation diagram of system state x versus the parameter b , for the control parameters $a = 0.25$, $c = 1$, $d = -0.45$, $e = -1$, $f = -1$ and $\alpha = 0.9$. It shows the huge importance of parameter b in creating a multi-wing attractor.

$$\alpha \frac{\pi}{2} < |\arg \lambda_i| \quad (i = 1, 2, 3). \tag{4.4}$$

The eigenvalues of $J(E_0)$ are given by $\lambda_{1,2,3} = d, e, a$ respectively. Hence, since $\lambda_{1,2,3}$ are all real numbers, a necessary condition for the origin $E_0 = (0, 0, 0)$ to be asymptotically stable is to have

$$d < 0, \quad e < 0 \quad \text{and} \quad a < 0. \tag{4.5}$$

Furthermore, the real character of $\lambda_{1,2,3}$ proves that there is no Hopf bifurcation anywhere near the origin.

The bifurcation diagram of the system (1.3) represented in both Figs. 1 and 2 show the symmetry of the chaotic attractors versus parameter b whose value at the centre is $b = 0$. This means that parameter b does not affect too much the chaos of the system but is particularly significant in generating a four-wing attractor.

5. Haar wavelets numerical method for the system 1.3

We analyze in this section the model 1.3

$$\begin{cases} D_t^\alpha x(t) = ax + cyz, \\ D_t^\alpha y(t) = bx + dy - xz, \\ D_t^\alpha z(t) = ez + fxy, \end{cases} \tag{5.1}$$

assumed to be subject to the following initial conditions

$$x(0) = u(x), \quad y(0) = v(y), \quad z(0) = w(z). \tag{5.2}$$

To transform the model (5.1) and (5.2) into a compact form, we define the following vectors for the system states

$$r(t) = \begin{pmatrix} x(t) \\ y(t) \\ z(t) \end{pmatrix} \quad \text{and} \quad g_0(x, y, z) = r(0) = \begin{pmatrix} x(0) \\ y(0) \\ z(0) \end{pmatrix} = \begin{pmatrix} u \\ v \\ w \end{pmatrix}$$

and the matrix operator

$$\begin{aligned} \mathcal{M}(r(t), t) &= \mathcal{M}(x(t), y(t), z(t), t) = \begin{pmatrix} \mathcal{M}_1(r(t), t) \\ \mathcal{M}_2(r(t), t) \\ \mathcal{M}_3(r(t), t) \end{pmatrix} \\ &= \begin{pmatrix} \mathcal{M}_1(x(t), y(t), z(t), t) \\ \mathcal{M}_2(x(t), y(t), z(t), t) \\ \mathcal{M}_3(x(t), y(t), z(t), t) \end{pmatrix} \end{aligned}$$

where

$$\begin{cases} \mathcal{M}_1(r(t), t) = ax + cyz, \\ \mathcal{M}_2(r(t), t) = bx + dy - xz, \\ \mathcal{M}_3(r(t), t) = ez + fxy \end{cases}$$

Hence, (5.1) becomes

$$\begin{aligned} D_t^\alpha r(t) &= \mathcal{M}(r(t), t) \\ \text{equivalently,} \\ D_t^\alpha x(t) &= \mathcal{M}_1(r(t), t) \\ D_t^\alpha y(t) &= \mathcal{M}_2(r(t), t) \\ D_t^\alpha z(t) &= \mathcal{M}_3(r(t), t) \end{aligned} \tag{5.3}$$

assumed to be subject to the following initial conditions

$$x(0) = u(x), \quad y(0) = v(y), \quad z(0) = w(z).$$

We can now make use of haar wavelets numerical scheme given in (3.6) to approximation the Caputo fractional derivative expressed-model (5.3) that yields

$$\begin{aligned} D_t^\alpha x(t) = \mathcal{M}_1(r(t), t) &\approx D_t^\alpha x_k(t) = {}^T C_{bk \times 1}^1 H_{bk \times 1} \\ D_t^\alpha y(t) = \mathcal{M}_2(r(t), t) &\approx D_t^\alpha y_k(t) = {}^T C_{bk \times 1}^2 H_{bk \times 1} \\ D_t^\alpha z(t) = \mathcal{M}_3(r(t), t) &\approx D_t^\alpha z_k(t) = {}^T C_{bk \times 1}^3 H_{bk \times 1} \end{aligned} \tag{5.4}$$

Applying the Rienmann–Liouville antiderivative (2.1) on both side of (5.4) yields

$$\begin{aligned} x(t) - u &\approx D_t^\alpha x_k(t) = {}^T C_{bk \times 1}^1 F_{bk \times bk}^\alpha H_{bk \times 1} \\ y(t) - v &\approx D_t^\alpha y_k(t) = {}^T C_{bk \times 1}^2 F_{bk \times bk}^\alpha H_{bk \times 1} \\ z(t) - w &\approx D_t^\alpha z_k(t) = {}^T C_{bk \times 1}^3 F_{bk \times bk}^\alpha H_{bk \times 1} \end{aligned} \tag{5.5}$$

equivalently

$$\begin{aligned} x(t) &\approx x_k(t) = {}^T C_{bk \times 1}^1 F_{bk \times bk}^\alpha H_{bk \times 1} + u \\ y(t) &\approx y_k(t) = {}^T C_{bk \times 1}^2 F_{bk \times bk}^\alpha H_{bk \times 1} + v \\ z(t) &\approx z_k(t) = {}^T C_{bk \times 1}^3 F_{bk \times bk}^\alpha H_{bk \times 1} + w \end{aligned} \tag{5.6}$$

where $F_{bk \times bk}^\alpha$ represents the haar wavelets fractional operational matrix [17,18]. Exploiting at this point the Galerkin’s method based on collocation points, in order to solve the model (5.1)–(5.2), the substitution of the approximated systems (5.4) and (5.6) into (5.1) generates the residual errors given by

$$\begin{aligned} e_1(\zeta^1, \zeta^2, \zeta^3, t) &= {}^T C_{bk \times 1}^1 H_{bk \times 1} - \mathcal{M}_1({}^T C_{bk \times 1}^1 F_{bk \times bk}^\alpha H_{bk \times 1}, \\ &\quad {}^T C_{bk \times 1}^2 F_{bk \times bk}^\alpha H_{bk \times 1}, {}^T C_{bk \times 1}^3 F_{bk \times bk}^\alpha H_{bk \times 1}, t) \\ e_2(\zeta^1, \zeta^2, \zeta^3, t) &= {}^T C_{bk \times 1}^2 H_{bk \times 1} - \mathcal{M}_2({}^T C_{bk \times 1}^1 F_{bk \times bk}^\alpha H_{bk \times 1}, \\ &\quad {}^T C_{bk \times 1}^2 F_{bk \times bk}^\alpha H_{bk \times 1}, {}^T C_{bk \times 1}^3 F_{bk \times bk}^\alpha H_{bk \times 1}, t) \\ e_3(\zeta^1, \zeta^2, \zeta^3, t) &= {}^T C_{bk \times 1}^3 H_{bk \times 1} - \mathcal{M}_3({}^T C_{bk \times 1}^1 F_{bk \times bk}^\alpha H_{bk \times 1}, \\ &\quad {}^T C_{bk \times 1}^2 F_{bk \times bk}^\alpha H_{bk \times 1}, {}^T C_{bk \times 1}^3 F_{bk \times bk}^\alpha H_{bk \times 1}, t) \end{aligned} \tag{5.7}$$

where

$$\begin{aligned} \zeta^1 &= c_{1,0}^1, \dots, c_{1,k-1}^1, \dots, c_{b,0}^1, \dots, c_{b,k-1}^1 \\ \zeta^2 &= c_{1,0}^2, \dots, c_{1,k-1}^2, \dots, c_{b,0}^2, \dots, c_{b,k-1}^2 \\ \zeta^3 &= c_{1,0}^3, \dots, c_{1,k-1}^3, \dots, c_{b,0}^3, \dots, c_{b,k-1}^3 \end{aligned}$$

with c_{\cdot}^i representing the components of ${}^T C_{\cdot \times \cdot}^i$.

Assuming that

$$\begin{aligned} e_1(\zeta^1, \zeta^2, \zeta^3, t_{s,i}) &= 0 \\ e_2(\zeta^1, \zeta^2, \zeta^3, t_{s,i}) &= 0 \\ e_3(\zeta^1, \zeta^2, \zeta^3, t_{s,i}) &= 0 \end{aligned}$$

where

$$t_{s,i} = \frac{2i-1}{2k} + s - 1, \quad s = 1, 2, \dots, b; \quad i = 1, 2, \dots, k$$

represent a bk number of collocation points, we finally obtain a system of $3bk$ equations, with $3bk$ unknowns given by

$$\begin{aligned} c_{1,0}^1, \dots, c_{1,k-1}^1, \dots, c_{b,0}^1, \dots, c_{b,k-1}^1 \\ c_{1,0}^2, \dots, c_{1,k-1}^2, \dots, c_{b,0}^2, \dots, c_{b,k-1}^2 \\ c_{1,0}^3, \dots, c_{1,k-1}^3, \dots, c_{b,0}^3, \dots, c_{b,k-1}^3 \end{aligned}$$

Therefore, we easily obtain these unknowns and substitution into (5.6) yields the desired approximated solution

$$r(t) \approx \begin{pmatrix} x_k(t) \\ y_k(t) \\ z_k(t) \end{pmatrix}$$

6. Convergence of the method through error analysis

Making use of error analysis, we present here exact error bounds that were used in the proposed numerical method to solve the model (5.1)–(5.2). For that since $r \in L^2[0, b]$, we assume that $x \in L^2[0, b]$, $y \in L^2[0, b]$ and $z \in L^2[0, b]$ and define

$$\|r\|_2 = (\|x\|_{L^2}^2 + \|y\|_{L^2}^2 + \|z\|_{L^2}^2)^{1/2} \tag{6.1}$$

where

$$\begin{aligned} \|x\|_{L^2} &= \left(\int_0^b |x(t)|^2 dt \right)^{1/2}, \quad \|y\|_{L^2} = \left(\int_0^b |y(t)|^2 dt \right)^{1/2}, \\ \|z\|_{L^2} &= \left(\int_0^b |z(t)|^2 dt \right)^{1/2}. \end{aligned}$$

Obviously $\|r\|_2$ represent a norm. From (3.5) and (3.6) we assume that similar to (5.6), the fractional derivative $D_t^\alpha r_k(t)$ is an approximation of $D_t^\alpha r(t)$ expressed as

$$D_t^\alpha r(t) \approx D_t^\alpha r_k(t) = \sum_{s=1}^b \sum_{i=0}^{k-1} c_{s,i} h_{s,i}(t)$$

Equivalently

$$\begin{pmatrix} D_t^\alpha x_k(t) \\ D_t^\alpha y_k(t) \\ D_t^\alpha z_k(t) \end{pmatrix} = D_t^\alpha r_k(t) = \sum_{s=1}^b \sum_{i=0}^{k-1} c_{s,i} h_{s,i}(t) = \begin{pmatrix} \sum_{s=1}^b \sum_{i=0}^{k-1} c_{s,i}^1 h_{s,i}(t) \\ \sum_{s=1}^b \sum_{i=0}^{k-1} c_{s,i}^2 h_{s,i}(t) \\ \sum_{s=1}^b \sum_{i=0}^{k-1} c_{s,i}^3 h_{s,i}(t) \end{pmatrix}$$

where $k \in \{2^j : j = 0, 1, 2, \dots\}$ and $c_{s,i} = \langle D_t^\alpha r_k, h_{s,i} \rangle_b = \int_0^b D_t^\alpha r_k(t) h_{s,i}(t) dt$,

$$\begin{aligned} c_{s,i}^1 &= \langle D_t^\alpha x_k, h_{s,i} \rangle_b = \int_0^b D_t^\alpha x_k(t) h_{s,i}(t) dt \\ c_{s,i}^2 &= \langle D_t^\alpha y_k, h_{s,i} \rangle_b = \int_0^b D_t^\alpha y_k(t) h_{s,i}(t) dt \\ c_{s,i}^3 &= \langle D_t^\alpha z_k, h_{s,i} \rangle_b = \int_0^b D_t^\alpha z_k(t) h_{s,i}(t) dt \end{aligned} \tag{6.2}$$

Hence,

$$\begin{aligned} D_t^\alpha r(t) - D_t^\alpha r_k(t) &= \sum_{s=1}^b \sum_{i=k}^\infty c_{s,i} h_{s,i}(t) \\ &= \sum_{s=1}^b \sum_{i=2^j}^\infty c_{s,i} h_{s,i}(t) \quad j = 0, 1, 2, \dots \\ &= \begin{pmatrix} \sum_{s=1}^b \sum_{i=2^j}^\infty c_{s,i}^1 h_{s,i}(t) \\ \sum_{s=1}^b \sum_{i=2^j}^\infty c_{s,i}^2 h_{s,i}(t) \\ \sum_{s=1}^b \sum_{i=2^j}^\infty c_{s,i}^3 h_{s,i}(t) \end{pmatrix} \quad j = 0, 1, 2, \dots \end{aligned} \tag{6.3}$$

Now, using the norm (6.1), we can state the following convergence results, that also hold for functions x, y and z in the Sobolev space $H^1[0, b]$.

Proposition 6.1. Let $0 \leq \alpha \leq 1$ and assume that $x \in H^1[0, b]$, $y \in H^1[0, b]$ and $z \in H^1[0, b]$. If the Caputo fractional derivative functions $D_t^\alpha r_k(t)$ are the approximations of $D_t^\alpha r(t)$ obtained via Haar wavelet schemes, then we have the exact upper bound reading as follows:

$$\|D_t^\alpha r(t) - D_t^\alpha r_k(t)\|_2 \leq \frac{K}{K_\alpha \Gamma(1-\alpha)} \tag{6.4}$$

where K is a real positive number and $K_\alpha = \frac{2(1-\alpha)}{b^{2\alpha}} \left(\frac{(3-3k^{(1-\alpha)})}{2^{2\alpha-2}} + \frac{(3-3k^{(2-2\alpha)})}{2^{2\alpha-4}} \right)^{-1/2}$.

Proof. From (6.1) and exploiting the haar wavelet expression (6.3) we have

$$\begin{aligned} \|D_t^\alpha r(t) - D_t^\alpha r_k(t)\|_2 &= (\|D_t^\alpha x - D_t^\alpha x_k\|_{L^2}^2 + \|D_t^\alpha y - D_t^\alpha y_k\|_{L^2}^2 + \|D_t^\alpha z - D_t^\alpha z_k\|_{L^2}^2)^{1/2} \\ &= \left(\int_0^b |D_t^\alpha x(t) - D_t^\alpha x_k(t)|^2 dt + \int_0^b |D_t^\alpha y(t) - D_t^\alpha y_k(t)|^2 dt \right. \end{aligned}$$

$$\begin{aligned}
 & + \int_0^b |D_t^\alpha z(t) - D_t^\alpha z_k(t)|^2 dt \Big)^{1/2} \\
 & = \left(\int_0^b \left| \sum_{s=1}^b \sum_{i=k}^\infty c_{s,i}^1 h_{s,i}(t) \right|^2 dt + \int_0^b \left| \sum_{s=1}^b \sum_{i=k}^\infty c_{s,i}^2 h_{s,i}(t) \right|^2 dt \right. \\
 & \quad \left. + \int_0^b \left| \sum_{s=1}^b \sum_{i=k}^\infty c_{s,i}^3 h_{s,i}(t) \right|^2 dt \right)^{1/2}.
 \end{aligned}$$

Using Fubini–Tonelli theorem for non-negative functions [36,37] and the fact that the family $\{h_i(t)\}_{i=0}^\infty$ forms a complete orthonormal system on $[0, b)$, that is, $\int_0^b H_{bk}(t)^T H_{bk}(t) dt = \mathbb{I}_{bk}$ (identity matrix),

$$\begin{aligned}
 & \|D_t^\alpha r(t) - D_t^\alpha r_k(t)\|_2 \\
 & \leq \left(\sum_{s=1}^b \sum_{j=0}^\infty \sum_{i=2^j}^{2^{j+1}} \int_0^b |c_{s,i}^1 h_{s,i}(t)|^2 dt + \sum_{s=1}^b \sum_{j=0}^\infty \sum_{i=2^j}^{2^{j+1}} \int_0^b |c_{s,i}^2 h_{s,i}(t)|^2 dt \right. \\
 & \quad \left. + \sum_{s=1}^b \sum_{j=0}^\infty \sum_{i=2^j}^{2^{j+1}} \int_0^b |c_{s,i}^3 h_{s,i}(t)|^2 dt \right)^{1/2} \\
 & \leq \left(\sum_{s=1}^b \sum_{j=0}^\infty \sum_{i=2^j}^{2^{j+1}} \int_0^b |c_{s,i}^1|^2 dt + \sum_{s=1}^b \sum_{j=0}^\infty \sum_{i=2^j}^{2^{j+1}} \int_0^b |c_{s,i}^2|^2 dt \right. \\
 & \quad \left. + \sum_{s=1}^b \sum_{j=0}^\infty \sum_{i=2^j}^{2^{j+1}} \int_0^b |c_{s,i}^3|^2 dt \right)^{1/2} \tag{6.5}
 \end{aligned}$$

where $c_{s,i}^q$, $q = 1, 2, 3$ are given in (6.2) and where we have considered the fact that k takes the form of powers of 2 ($k \in \{2^j : j = 0, 1, 2, \dots\}$).

Now computing each $c_{s,i}^q$ using (6.2), the definitions (3.2) and (3.3) of $h_{s,i}$ imply

$$\begin{aligned}
 c_{s,i}^1 &= (\sqrt{2})^j \left[\int_{\frac{k}{2^j}-1+s}^{\frac{k+\frac{1}{2}}{2^j}-1+s} D_t^\alpha x(t) dt - \int_{\frac{k+1}{2^j}-1+s}^{\frac{k+\frac{1}{2}}{2^j}-1+s} D_t^\alpha x(t) dt \right] \\
 c_{s,i}^2 &= (\sqrt{2})^j \left[\int_{\frac{k}{2^j}-1+s}^{\frac{k+\frac{1}{2}}{2^j}-1+s} D_t^\alpha y(t) dt - \int_{\frac{k+1}{2^j}-1+s}^{\frac{k+\frac{1}{2}}{2^j}-1+s} D_t^\alpha y(t) dt \right] \\
 c_{s,i}^3 &= (\sqrt{2})^j \left[\int_{\frac{k}{2^j}-1+s}^{\frac{k+\frac{1}{2}}{2^j}-1+s} D_t^\alpha z(t) dt - \int_{\frac{k+1}{2^j}-1+s}^{\frac{k+\frac{1}{2}}{2^j}-1+s} D_t^\alpha z(t) dt \right]
 \end{aligned} \tag{6.6}$$

Using the Mean value theorem for definite integrals, there are two times $\tau_x \in (\frac{k}{2^j} - 1 + s, \frac{k+\frac{1}{2}}{2^j} - 1 + s)$ and $\tilde{\tau}_x \in (\frac{k+1}{2^j} - 1 + s, \frac{k+\frac{1}{2}}{2^j} - 1 + s)$ such that

$$\begin{aligned}
 c_{s,i}^1 &= (\sqrt{2})^j \left(\frac{1}{2^{j+1}} D_t^\alpha x(\tau_x) dt - \frac{1}{2^{j+1}} D_t^\alpha x(\tilde{\tau}_x) dt \right) \\
 &= 2^{-(\frac{j}{2}+1)} (D_t^\alpha x(\tau_x) dt - D_t^\alpha x(\tilde{\tau}_x) dt)
 \end{aligned} \tag{6.7}$$

Using the formulation (2.3) of Caputo derivative leads to

$$\begin{aligned}
 |c_{s,i}^1| &= 2^{-(\frac{j}{2}+1)} |D_t^\alpha x(\tau_x) dt - D_t^\alpha x(\tilde{\tau}_x) dt| \\
 &= 2^{-(\frac{j}{2}+1)} \frac{1}{\Gamma(1-\alpha)} \left| \int_0^{\tau_x} (\tau_x - \xi)^{-\alpha} \frac{dx(\xi)}{d\xi} d\xi \right. \\
 & \quad \left. - \int_0^{\tilde{\tau}_x} (\tilde{\tau}_x - \xi)^{-\alpha} \frac{dx(\xi)}{d\xi} d\xi \right|
 \end{aligned}$$

Since $x \in H^1[0, b)$, hence there is a positive constant \mathcal{K}_x such that $\|\dot{x}(\xi)\| \leq \mathcal{K}_x$ for all $\xi \in (0, \tau_x)$ and $\xi \in (0, \tilde{\tau}_x)$. This yields

$$|c_{s,i}^1| \leq \mathcal{K}_x 2^{-(\frac{j}{2}+1)} \frac{1}{\Gamma(1-\alpha)} \left| \int_0^{\tau_x} (\tau_x - \xi)^{-\alpha} d\xi - \int_0^{\tilde{\tau}_x} (\tilde{\tau}_x - \xi)^{-\alpha} d\xi \right|$$

Integrating and simplifying finally lead to

$$\begin{aligned}
 |c_{s,i}^1| &\leq \frac{\mathcal{K}_x 2^{-(\frac{j}{2}+1)}}{(1-\alpha)\Gamma(1-\alpha)} |\tau_x^{(1-\alpha)} - (\tilde{\tau}_x)^{(1-\alpha)}| \\
 &\leq \frac{\mathcal{K}_x 2^{-(\frac{j}{2}+1)}}{(1-\alpha)\Gamma(1-\alpha)} 2^{j(1-\alpha)},
 \end{aligned} \tag{6.8}$$

where we have used the facts that $0 \leq \alpha \leq 1$, $\tau_x \in (\frac{k}{2^j} - 1 + s, \frac{k+\frac{1}{2}}{2^j} - 1 + s)$ and $\tilde{\tau}_x \in (\frac{k+1}{2^j} - 1 + s, \frac{k+\frac{1}{2}}{2^j} - 1 + s)$.

In a similar way, we prove easily that there are positive constants \mathcal{K}_y and \mathcal{K}_z such that

$$|c_{s,i}^2| \leq \frac{\mathcal{K}_y 2^{-(\frac{j}{2}+1)}}{(1-\alpha)\Gamma(1-\alpha)} 2^{j(1-\alpha)} \tag{6.9}$$

and

$$|c_{s,i}^3| \leq \frac{\mathcal{K}_z 2^{-(\frac{j}{2}+1)}}{(1-\alpha)\Gamma(1-\alpha)} 2^{j(1-\alpha)}. \tag{6.10}$$

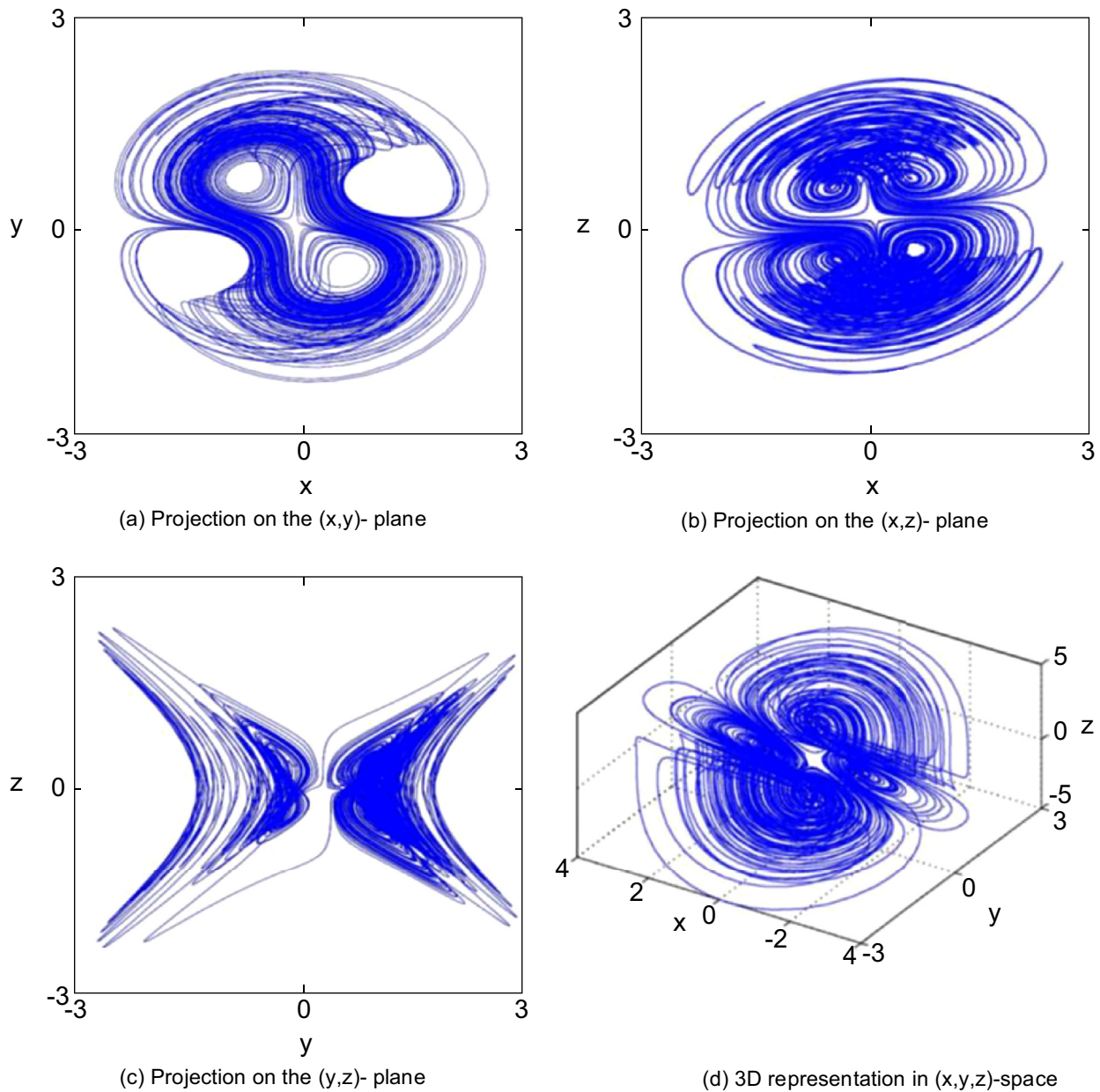
Define $K = \max(\mathcal{K}_x, \mathcal{K}_y, \mathcal{K}_z)$. The substitution of (6.8), (6.9) and (6.10) into (6.5) gives

$$\begin{aligned}
 & \|D_t^\alpha r(t) - D_t^\alpha r_k(t)\|_2 \\
 & \leq \left(\frac{3bK^2}{4(\Gamma(1-\alpha))^2(1-\alpha)^2} \sum_{s=1}^b \sum_{j=0}^\infty \sum_{i=2^j}^{2^{j+1}} \frac{2^{2j(1-\alpha)}}{2^j} \right)^{1/2} \\
 & \leq \left(\frac{3b^2K^2}{4(\Gamma(1-\alpha))^2(1-\alpha)^2} \right. \\
 & \quad \left. \times \left(\frac{2^{2\alpha} - 2^{2\alpha}k^{(1-\alpha)}}{2^{2\alpha} - 2} + \frac{2^{2\alpha} - 2^{2\alpha}k^{(2-2\alpha)}}{2^{2\alpha} - 4} \right) \right)^{1/2} \\
 & \leq \frac{bK}{2(\Gamma(1-\alpha))(1-\alpha)} \left(3 \frac{2^{2\alpha}(1-k^{(1-\alpha)})}{2^{2\alpha} - 2} + 3 \frac{2^{2\alpha}(1-k^{(2-2\alpha)})}{2^{2\alpha} - 4} \right)^{1/2}
 \end{aligned} \tag{6.11}$$

Which ends the proof. \square



Fig. 3. Rough representation of a four-scroll attractor of system (1.3) in a chaotic state, with the control parameters $a = 4, b = 1, c = 5, d = 5, e = 10, f = 1$ and $\alpha = 1.0$.



$\alpha=1$

Fig. 4. Chaotic attractor with four wings generated by system (1.3), with the control parameters $a = 0.25$, $c = 1$, $d = -0.45$, $e = -1$, $f = -1$ and $\alpha = 1.0$. The chaos is shown to be governed by a fractal structure.

Remark 6.1. If the functions x , y and z do not belong to $H^1[0, b)$ then the only condition $x \in L^2[0, b)$, $y \in L^2[0, b)$ and $z \in L^2[0, b)$ is not enough to state the Proposition 6.1 since the interval $[0, b)$ is not closed. Hence the functions x , y , z and their first order derivatives might not be bounded nor attain their bounds on $[0, b)$.

Hence we have proved the following

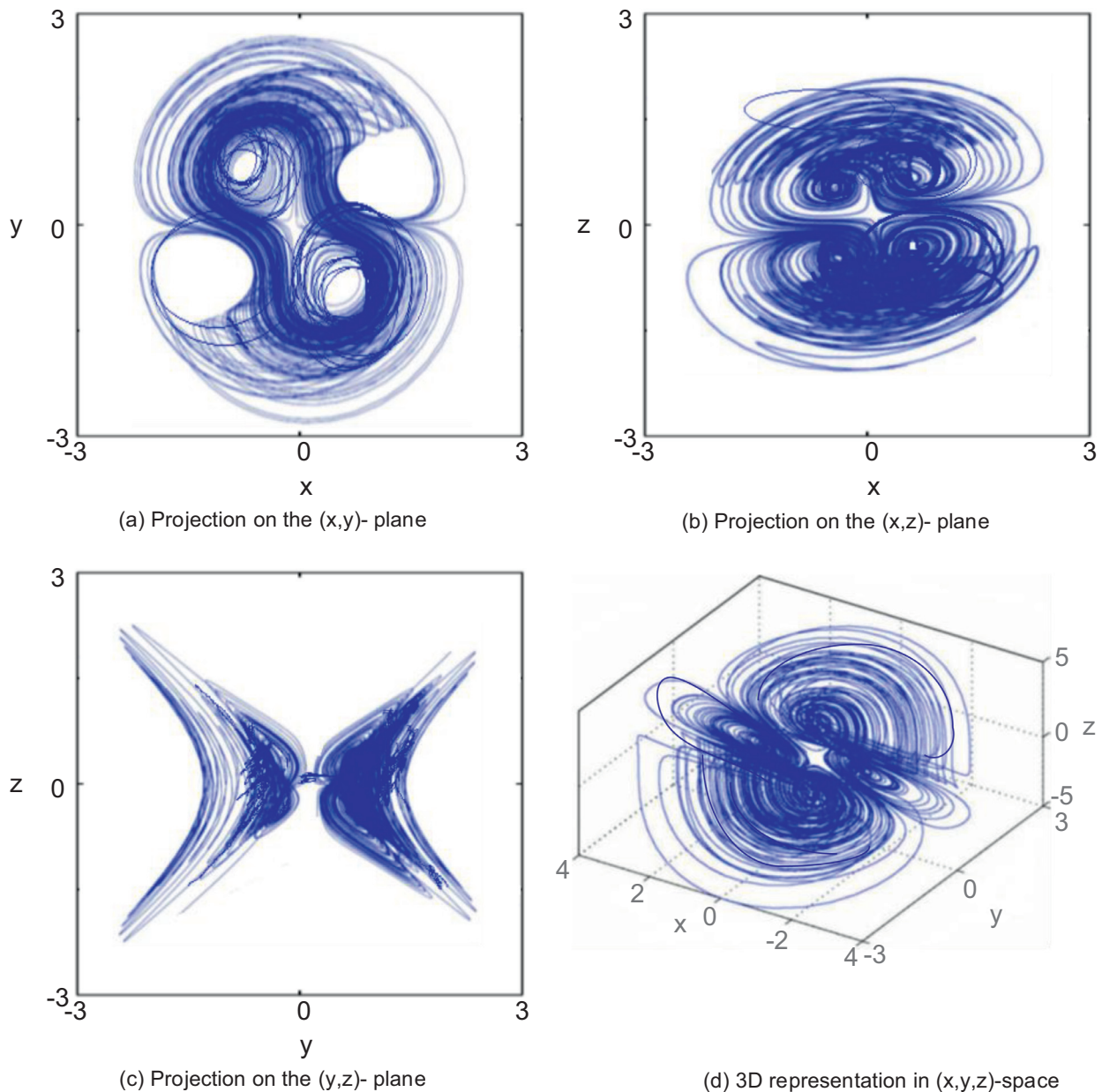
Corollary 6.1. Let $0 \leq \alpha \leq 1$, $x \in L^2[0, b)$, $y \in L^2[0, b)$, $z \in L^2[0, b)$ and assume that $\dot{x}(t)$, $\dot{y}(t)$ and $\dot{z}(t)$ are continuous and bounded on $[0, b)$. If the Caputo fractional derivative functions $D_t^\alpha r_k(t)$ are the approximations of $D_t^\alpha r(t)$ obtained via Haar wavelet schemes, then we have the exact upper bound reading as follows:

$$\|D_t^\alpha r(t) - D_t^\alpha r_k(t)\|_2 \leq \frac{K}{K_\alpha \Gamma(1 - \alpha)} \tag{6.12}$$

where K is a real positive number and $K_\alpha = \frac{2(1-\alpha)}{b^{2\alpha}} \left(\frac{(3-3k^{(1-\alpha)})}{2^{2\alpha-2}} + \frac{(3-3k^{(2-2\alpha)})}{2^{2\alpha-4}} \right)^{-1/2}$.

7. Simulations and attractor representations

Now that the error committed by using Haar wavelets scheme in our context has been successfully analyzed and shown to be insubstantial, we can provide numerical simulations using the scheme presented above. It appears here that the model (1.3), solved using the Haar wavelets is chaotic as expected (see Figs. 3–5). Fig. 3 exhibits a crude representation of a four-scroll chaotic attractor of the system (1.3) for the control parameters $a = 4$, $b = 1$, $c = 5$, $d = 5$, $e = 10$, $f = 1$. The same analysis is done for Figs. 4 and 5 but this time, for the control parameters $a =$



$$\alpha=0.9$$

Fig. 5. Chaotic attractor with four wings generated by system (1.3), with the control parameters $a = 0.25$, $c = 1$, $d = -0.45$, $e = -1$, $f = -1$ and $\alpha = 0.9$. Again the chaos is shown to be governed by a fractal structure.

0.25 , $c = 1$, $d = -0.45$, $e = -1$, $f = -1$. The processes in both regular case ($\alpha = 1$) and pure fractional case ($\alpha = 0.9$) show chaotic dynamics. One of the particularities here is the appearance in those figures of two types of attractors: a global orbital and dynamical attractor and a local one. The global attractor does not count on the initial zones of the orbit. It is characterized by complex orbits around all the equilibrium points and also represented as a double-scroll and four-scroll chaotic attractor. The local attractor does count on the initial zones of the orbit and characterized by a sink, basic periodic orbits and a single-scroll chaotic attractor (Figs. 4–5). The values of the control parameter α on top of the other ones (a , b , c , d , e , f) provides additional options for modulating the system and hence, represents an extra ingredient in this powerful recipe for the generation and control of chaotic dynamics with strange attractors.

8. Concluding remarks

We have used the Haar wavelet numerical method to analyze a three-dimensional system of Caputo fractional differential equations. The system is proved to generate chaotic four-wing attractors. Equilibrium points have been studied and conditions of stability of the trivial equilibrium point (the origin) are provided for our model. The error analysis has been performed and has shown that the Haar wavelet method is convergent in the context and conditions of our analysis. Graphical simulations have been performed for two values of the parameter α and all exhibit existence of a chaotic system characterized by orbits with four scrolls, which is specific to strange attractors. This is the first instance where a model of Caputo fractional differential equations of type (1.3) is solved using a relatively recent method like wavelet

method. Hence, the Haar wavelets scheme combined with the Caputo fractional derivative appears to be a powerful tool in generating and modulating strange and chaotic multi-wing attractors.

Acknowledgments

This work was partially supported by the grant No. 105932 from the National Research Foundation (NRF) South Africa and a grant from the Simons Foundation.

References

- [1] Atangana A, Nieto J. Numerical solution for the model of rlc circuit via the fractional derivative without singular kernel. *Adv Mech Eng* 2015;7(10):1–7.
- [2] Brockmann D, Hufnagel L. Front propagation in reaction-superdiffusion dynamics: taming lévy flights with fluctuations. *Phys Rev Lett* 2007;98(17):178301.
- [3] Doungmo Goufo EF. Speeding up chaos and limit cycles in evolutionary language and learning processes. *Math Methods Appl Sci* 2016;inpress.
- [4] Doungmo Goufo EF. Application of the Caputo-Fabrizio fractional derivative without singular kernel to korteweg-de vries-bergers equation. *Math Modell Anal* 2016;21(2):188–98.
- [5] Das S. Convergence of riemann-liouville and caputo derivative definitions for practical solution of fractional order differential equation. *Int J Appl Math Stat* 2011;23(D11):64–74.
- [6] Hilfer R. *Application of fractional calculus in physics*. World Scientific, Singapore; 1999.
- [7] Kilbas AAA, Srivastava HM, Trujillo JJ. *Theory and applications of fractional differential equations*, 204. Elsevier Science Limited; 2006.
- [8] Pooseh S, Rodrigues HS, Torres DF. Fractional derivatives in dengue epidemics. In: *AIP Conference Proceedings*, 1389. AIP; 2011. p. 739–42.
- [9] Yang X-J, Srivastava H, He J-H, Baleanu D. Cantor-type cylindrical-coordinate method for differential equations with local fractional derivatives. *Phys Lett A* 2013;377(28):1696–700.
- [10] Atangana A. On the stability and convergence of the time-fractional variable order telegraph equation. *J Comput Phys* 2015;293:104–14.
- [11] Doungmo Goufo EF, Atangana A. Analytical and numerical schemes for a derivative with filtering property and no singular kernel with applications to diffusion. *Eur Phys J Plus* 2016;131(8):269.
- [12] Doungmo Goufo EF. Stability and convergence analysis of a variable order replicator-mutator process in a moving medium. *J Theor Biol* 2016;403:178–87.
- [13] El-Kalla I. Convergence of the adomian method applied to a class of nonlinear integral equations. *Appl Math Lett* 2008;21(4):372–6.
- [14] Odibat ZM. A study on the convergence of variational iteration method. *Math Comput Model* 2010;51(9):1181–92.
- [15] Podlubny I. *Fractional differential equations*. Academic Press, New York; 1999.
- [16] Lepik Ü, Hein H. *Haar wavelets: with applications*. Springer Science & Business Media; 2014.
- [17] Babolian E, Shamsavaran A. Numerical solution of nonlinear fredholm integral equations of the second kind using haar wavelets. *J Comput Appl Math* 2009;225(1):87–95.
- [18] Chen Y, Yi M, Yu C. Error analysis for numerical solution of fractional differential equation by haar wavelets method. *J Comput Sci* 2012;3(5):367–73.
- [19] Boeing G. Visual analysis of nonlinear dynamical systems: chaos, fractals, self-similarity and the limits of prediction. *Systems* 2016;4(4):37.
- [20] Liu C, Liu T, Liu L, Liu K. A new chaotic attractor. *Chaos, Solitons Fractals* 2004;22(5):1031–8.
- [21] Zaslavsky G. The simplest case of a strange attractor. *Phys Lett A* 1978;69(3):145–7.
- [22] Lorenz EN. Deterministic nonperiodic flow. *J Atmos Sci* 1963;20(2):130–41.
- [23] Rössler OE. An equation for continuous chaos. *Phys Lett A* 1976;57(5):397–8.
- [24] Hénon M. A two-dimensional mapping with a strange attractor. *Commun Math Phys* 1976;50(1):69–77.
- [25] Arneodo A, Coulet P, Tresser C. Possible new strange attractors with spiral structure. *Commun Math Phys* 1981;79(4):573–9.
- [26] Lü J, Chen G. Generating multiscroll chaotic attractors: theories, methods and applications. *Int J Bifurcation Chaos* 2006;16(04):775–858.
- [27] Doungmo Goufo EF. Chaotic processes using the two-parameter derivative with non-singular and non-local kernel: basic theory and applications. *Chaos* 2016;26(8):084305.
- [28] Wang Z, Sun Y, van Wyk BJ, Qi G, van Wyk MA. A 3-d four-wing attractor and its analysis. *Braz J Phys* 2009;39(3):547–53.
- [29] Zhou T, Chen G. Classification of chaos in 3-d autonomous quadratic systems-i: basic framework and methods. *Int J Bifurcation Chaos* 2006;16(09):2459–79.
- [30] Caputo M. Linear models of dissipation whose q is almost frequency independent-II. *Geophys J Int* 1967;13(5):529–39.
- [31] Caputo M, Fabrizio M. A new definition of fractional derivative without singular Kernel. In: *Progress in fractional differentiation and applications*; 2015. p. 73–85.
- [32] Losada J, Nieto J. Properties of the new fractional derivative without singular kernel. *Progr Fract Differ Appl* 2015;1(2):87–92.
- [33] Atangana A, Baleanu D. New fractional derivatives with non-local and non-singular kernel. *Thermal Sci* 2016;20(2):763–9.
- [34] Čelikovský S, Chen G. On the generalized lorenz canonical form. *Chaos, Solitons Fractals* 2005;26(5):1271–6.
- [35] Matignon D. Stability results for fractional differential equations with applications to control processing. In: *Computational engineering in systems applications*, vol. 2. IMACS, IEEE-SMC Lille, France; 1996. p. 963–8.
- [36] Tonelli L. Sull'Integrazione per parti. *Rend Acc Naz Lincei* 1909;5(18):246–53.
- [37] Fubini G. *Opere scelte*, vol. 2. Cremonese; 1958.